Acta Biomaterialia 49 (2017) 1–15

Contents lists available at ScienceDirect

Acta Biomaterialia

journal homepage: www.elsevier.com/locate/actabiomat

Review article

Extracellular matrix hydrogels from decellularized tissues: Structure and function

Lindsey T. Saldin [a,b,1], Madeline C. Cramer [a,b,1], Sachin S. Velankar [c], Lisa J. White [b,d], Stephen F. Badylak [a,b,e,*]

[a] Department of Bioengineering, University of Pittsburgh, 360B CNBIO, 300 Technology Drive, Pittsburgh, PA 15219, USA
[b] McGowan Institute for Regenerative Medicine, Suite 300, 450 Technology Drive, University of Pittsburgh, Pittsburgh, PA 15219, USA
[c] Department of Chemical Engineering, University of Pittsburgh, 940 Benedum Hall, Pittsburgh, PA 15261, USA
[d] School of Pharmacy, University of Nottingham, University Park, Nottingham NG7 2RD, UK
[e] Department of Surgery, University of Pittsburgh, 200 Lothrop Street, Pittsburgh, PA 15213, USA

ARTICLE INFO

Article history:
Received 6 October 2016
Received in revised form 11 November 2016
Accepted 30 November 2016
Available online 1 December 2016

Keywords:
Extracellular matrix
Hydrogel
Decellularization
Naturally derived
Injectable
Regenerative medicine
Biomaterial
Tissue engineering

ABSTRACT

Extracellular matrix (ECM) bioscaffolds prepared from decellularized tissues have been used to facilitate constructive and functional tissue remodeling in a variety of clinical applications. The discovery that these ECM materials could be solubilized and subsequently manipulated to form hydrogels expanded their potential *in vitro* and *in vivo* utility; i.e. as culture substrates comparable to collagen or Matrigel, and as injectable materials that fill irregularly-shaped defects. The mechanisms by which ECM hydrogels direct cell behavior and influence remodeling outcomes are only partially understood, but likely include structural and biological signals retained from the native source tissue. The present review describes the utility, formation, and physical and biological characterization of ECM hydrogels. Two examples of clinical application are presented to demonstrate *in vivo* utility of ECM hydrogels in different organ systems. Finally, new research directions and clinical translation of ECM hydrogels are discussed.

Statement of Significance

More than 70 papers have been published on extracellular matrix (ECM) hydrogels created from source tissue in almost every organ system. The present manuscript represents a review of ECM hydrogels and attempts to identify structure-function relationships that influence the tissue remodeling outcomes and gaps in the understanding thereof. There is a Phase 1 clinical trial now in progress for an ECM hydrogel.

Contents

* Corresponding author at: Suite 300, 450 Technology Drive, Pittsburgh, PA 15219, USA.
E-mail addresses: saldinlt@upmc.edu (L.T. Saldin), cramerm2@upmc.edu (M.C. Cramer), velankar@pitt.edu (S.S. Velankar), lisa.white@nottingham.ac.uk (L.J. White), badylaks@upmc.edu (S.F. Badylak).
[1] These authors contributed equally to this work.

http://dx.doi.org/10.1016/j.actbio.2016.11.068
1742-7061/

1. Introduction

Hydrogels are defined as highly hydrated polymer materials (>30% water by weight), which maintain structural integrity by physical and chemical crosslinks between polymer chains [1]. The polymer chains can be synthetic [e.g., polyethylene oxide (PEO), poly(vinyl alcohol) (PVA), poly(acrylic acid) (PAA), poly(pro pylenefumarate-co-ethylene glycol) P(PF-co-EG)] or natural (e.g., alginate, chitosan, collagen, hyaluronic acid). Synthetic and natural hydrogels have been widely used to fill space, deliver bioactive molecules/drugs, and/or deliver cells to stimulate tissue growth [1].

Many hydrogels have been derived from components of the extracellular matrix (ECM) such as collagen, hyaluronic acid and elastin or complex mixtures of ECM proteins such as Matrigel. The focus of the present review is ECM hydrogels and specifically, hydrogels that are 1) derived from decellularized mammalian tissue, and 2) enzymatically solubilized and neutralized to physiologic pH and temperature. Hence, ECM materials that fulfill one of these criteria, such as decellularized tissues that are "gel-like" but not further solubilized (for example decellularized human lipoaspirate [2], intervertebral disc [3,4], and devitalized cartilage [5,6]) are beyond the scope of this review. In contrast to hydrogels composed of individual ECM components, ECM hydrogels retain the full biochemical complexity of the native tissue, and unlike Matrigel, are not composed of a protein source that is a product of a tumorigenic cell line.

To date, ECM hydrogels have been primarily used as 3D organotypic culture models and to stimulate tissue growth after injury. The present review describes the utility, formation and physical and biological characterization of ECM hydrogels. Two examples of clinical application in selected organ systems are presented. Finally, new research directions and clinical translation of ECM hydrogels are discussed.

1.1. Why ECM?

The ECM consists of the structural and functional molecules secreted by the resident cells of each tissue, hence the 3D organization and biochemical composition of the ECM is distinctive for each tissue type. ECM has been influencing cell behavior, dynamically and reciprocally [7] since single cell organisms evolved more than 600 million years ago, and likely played a central role in the transition from unicellular organisms to multicellular organisms [8]. Mimicking aspects of the structure and composition of the ECM has guided the rational design of biomaterials over the past several decades in attempts to proactively influence cell behavior [9].

Although decellularization of tissue was first reported in 1973 as a technique to preserve tissue intended to be used as a protective barrier for burn patients [10], the first reported production of ECM by decellularization of a source tissue for subsequent use as a bioscaffold for tissue reconstruction was the use of small intestinal submucosa (SIS) for vascular applications [11–15]. These initial studies removed cellular material while preserving the structural and functional proteins of the ECM such as glycosaminoglycans (GAGs), proteoglycans, and growth factors [16]. When processed appropriately, ECM materials harvested by such methods retain the biochemical complexity, nanostructure, and bioinductive properties of the native matrix, and have been shown to promote the *in vivo* creation of site-specific, functional tissue [17]. ECM-derived materials are FDA-allowed, can be preserved and used 'off the shelf,' have been implanted in millions of patients to date; and have been extensively characterized in both the 2D sheet and powder forms [17,18].

The discovery that ECM bioscaffolds could be transformed into hydrogels expanded their potential *in vitro* and *in vivo* utility [16]. For example, minimally invasive delivery becomes possible wherein a pre-gel viscous fluid is injected with a catheter or syringe and polymerizes at physiologic temperature into a hydrogel conforming to the shape of any defect site. Compared to suspensions of ECM powders, ECM hydrogels can be injected with a more homogenous concentration and with greater ease [19].

Hydrogels derived from SIS and urinary bladder matrix (UBM) have been shown to retain the inherent bioactivity of the native matrix with the ability to promote constructive remodeling in heterologous tissue applications [16,20–26]. In the last decade more than 70 papers have been published on the use of ECM hydrogels in almost every organ system. The mechanisms by which the ECM hydrogel modulates cell behavior are not fully understood but likely include release of bound growth factors [27], cytokines, and chemokines [28], presentation of cryptic peptides [29–32], exposure of bioactive motifs, and as recently reported, through bioactive matrix-bound nanovesicles [33].

2. ECM hydrogel formation

ECM hydrogel formation is a collagen-based self-assembly process that is regulated in part by the presence of glycosaminoglycans, proteoglycans, and ECM proteins [34]. Therefore, polymerization kinetics will be influenced by the native biochemical profile of the source tissue and of the proteins that remain after decellularization and solubilization. It is important to achieve sufficient cell removal from source tissues [35,36] while maintaining ECM composition and ultrastructure. The choice of solubilization protocol is crucial to not adversely affect the ability to subsequently form an ECM hydrogel. Table 1 provides an overview of the many methods used to decellularize source tissues and solubilize the remaining ECM. ECM hydrogels are primarily derived from porcine tissue but some hydrogel types, e.g., adipose, tendon, umbilical cord are sourced from human tissue.

Formation of a hydrogel involves two key steps: 1) solubilization of the ECM material into protein monomeric components, and 2) temperature- and/or pH-controlled neutralization to induce spontaneous reformation of the intramolecular bonds of the monomeric components into a homogeneous gel. The most prevalent method used to form an ECM hydrogel is via pepsin mediated solubilization of a comminuted (powder) form of ECM (also called "ECM digestion"). Pepsin is an enzyme derived from porcine gastric juices that has been used since 1972 to solubilize a substantial

Table 1
Decellularization reagents and solubilization protocol used to produce ECM hydrogels for each source tissue and species. The fundamental solubilization protocols are referred to as Voytik-Harbin, Freytes and Uriel as defined below. Any modifications to the base protocol are indicated within the table.

Source Tissue	Decellularization Reagents	Solubilization Protocol	Ref.
Adipose			
Human *(Lipoaspirate)*	• 1% SDS, or 2.5 mM sodium deoxycholate • 2.5 mM sodium deoxycholate with 500 U lipase and 500 U colipase	• Freytes • 3200 IU pepsin • 0.1 M HCl	[67]
	• 0.5% SDS • Isopropanol • 0.1% peracetic acid/4% ethanol	• Voytik-Harbin • 10 mg pepsin • RT, 48 h	[73]
Rat *(Subcutaneous)*	• 2 mL dispase/g tissue ⌘	• Uriel	[43,44,47]
Porcine	• 10 mM Tris and 5 mM EDTA • 99% isopropanol • HBSS with 10,000 U DNase, 12.5 mg RNase, 1000 U lipase	• Freytes • 37 °C, 24 h	[97]
Bone			
Bovine *(Cancellous Tibia)*	• 0.5 M HCl • 1:1 Chloroform:methanol • 0.05% trypsin/0.02% EDTA • 1% w/v pen/strep in PBS	• Freytes • 96 h	[72,86,98]
Cartilage			
Porcine *(Articular)*	• 10 mM Tris-HCl at pH 8 • 0.25% trypsin • 1.5 M NaCl in 50 mM Tris-HCl at pH 7.6 • 50 U/mL DNase and 1 U/mL RNase in 10 mM Tris-HCl • 1% Triton X-100 • 10 mM Tris-HCl • 0.1% peracetic acid/4% ethanol	• Voytik-Harbin • 10 mg pepsin • RT, 48 h	[73]
Porcine *(Meniscus)*	• 1% SDS • 0.1% EDTA	• Freytes • 1.5 mg/mL pepsin	[70]
Central Nervous System			
Porcine *(Adult Brain, Spinal Cord)*	• 0.02% trypsin/0.05% EDTA • 3% Triton X-100 • 1 M sucrose • 4% deoxycholate • 0.1% peracetic acid/4% ethanol	• Freytes	[54,82,91,99]
Porcine *(Fetal Brain)*	• 0.05% trypsin-EDTA with 0.2% DNase I • 3% Triton X-100 with 0.2% DNase I • 1 M sucrose • 1% sodium deoxycholate • 0.2% peracetic acid in 4% ethanol	• Freytes • 24 h	[100]
Colon			
Porcine *(Submucosa)*	• 2:1 Chloroform:methanol • Graded ethanol (100%, 90%, 70%) • 0.02% trypsin/0.05% EDTA • 4% sodium deoxycholate • 0.1% peracetic acid/4% ethanol	• Freytes • 0.1 M HCl	[71]
Cornea			
Porcine	• 10 U/ml DNAse and 10 U/mL RNAse in 10 nM MgCL2	• Freytes • 0.1 M HCl • 72 h	[69]

(*continued on next page*)

Table 1 (*continued*)

Source Tissue	Decellularization Reagents	Solubilization Protocol	Ref.
Esophagus			
Porcine *(Mucosa/submucosa)*	• 1% trypsin/0.05% EDTA • 1 M sucrose • 3% Triton X-100 • 10% deoxycholate • 0.1% peracetic acid/4% ethanol	• Freytes	[101]
Heart			
Porcine, Rat *(Ventricular Myocardium)*	• 1% SDS • 1% Triton X-100	• Freytes • 0.1 M HCl	[58,74,75,77,79,81,102]
Porcine *(Ventricular Myocardium)*	• 1% SDS and 0.5% pen/strep	• Freytes • 0.1 M HCl	[42,60,80,103–106]
	• 1% SDS • 1% Triton X-100 • 0.1% peracetic acid/4% ethanol	• Voytik-Harbin • 10 mg pepsin • RT, 48 h	[73,107]
	• 0.02% trypsin-EDTA • 3% Tween-20 • 102 mM sodium deoxycholate • 0.1% peracetic acid • 1% pen/strep	• Freytes	[108]
	• 1% SDS • 0.1% Triton X-100	• Freytes • 0.1 M HCl • 12 h	[109]
	Perfusion • 0.02% trypsin/0.05% EDTA • 3% Triton X-100/0.05% EDTA • 4% deoxycholic acid • 0.1% peracetic acid • 2:1 chloroform:methanol • 100–70% ethano	• Freytes • 2 mg/mL pepsin	[110]
Human *(Ventricular Myocardium)*	• 1% SDS and 0.5% pen/strep • Isopropyl alcohol • 40 U/mL DNase and 1 U/mL RNase in 40 mM HCl, 6 mM MgCl2, 1 mM CaCl2, and 10 mM NaCl • 1% SDS/0.5% pen/strep • 0.001% Triton X-100	• Freytes	[60]
	• 10 mM Tris and 0.1% EDTA • 0.5% SDS • 100 U/mL pen/strep and nystatin in DPBS • Fetal bovine serum • 100 U/mL pen/strep and nystatin in DPBS	• Freytes • pH 1 • 37 °C • Salts were not neutralized	[111]
	• 10 mM Tris and 0.1% EDTA • 0.5% SDS • 100 U/mL pen/strep and nystatin in DPBS • Fetal bovine serum • 100 U/mL pen/strep and nystatin in DPBS	• Freytes • pH 2	[111]
Goat *(Ventricle)*	• 0.1% peroxyacetic acid/4% ethanol • 1% SDS • 1% Triton X-100	• Freytes • 60–72 h	[112]
Porcine, Human *(Pericardium)*	• 1% SDS	• Freytes • 0.1 M HCl	[55,76,78,94,113]
Kidney			
Human *(Cortex)*	• 1% SDS	• Freytes	[61]

Table 1 (*continued*)

Source Tissue	Decellularization Reagents	Solubilization Protocol	Ref.
Liver			
Rat	*Perfusion* • 1% Triton X-100 and 0.1% ammonium hydroxide	• Freytes • 10% (w/w) pepsin • 0.1 M HCl	[57]
Rat, Porcine, Canine, Human	• 0.02% trypsin and 0.05% EGTA • 3% Triton X-100 • 0.1% peracetic acid	• Freytes • 24–72 h (until no particulate)	[56]
Porcine	• 0.02% trypsin and 0.05% EDTA • 3% Triton X-100 • 4% sodium deoxycholic acid • 0.1% peracetic acid	• Freytes • 72 h	[87,88]
	• 0.1% SDS	• Freytes • 3 mg/mL pepsin • 0.1 M HCl • 72 h	[52]
Lung			
Porcine	*Perfusion* • 1x pen/strep • 0.1% Triton X-100 • 2% sodium deoxycholate • DNase solution • NaCl	• Freytes	[49]
Pancreas			
Porcine	• 1.1% NaCl • 0.7% NaCl • 0.05% trypsin/0.02% EDTA, pH 8.2 • 1% Triton X-100/1% ammonium hydroxide • 70% ethanol	• Freytes • 5 mg/mL pepsin • 0.1 M HCl	[62]
Skeletal Muscle			
Porcine *(Intercostal, Hindleg)*	• 1% SDS	• Freytes • 0.1 M HCl	[58,83]
Porcine *(Psoas)*	• 1% SDS • 1% SDS and 0.5% pen/strep • Isopropyl alcohol	• Freytes • 0.1 M HCl	[104]
	• 1% SDS and 0.5% pen/strep • Isopropyl alcohol • 0.001% Triton X-100	• Freytes • 0.1 M HCl	[63]
Porcine	• 0.2% trypsin/0.1% EDTA • 0.5% Triton X-100 • 1% Triton X-100/ 0.2% sodium deoxycholate • Isopropanol • 5x107 U/l DNase-I and 1x106 U/l RNase	• Freytes	[64]
Skin			
Rat *(Dermis)*	• 2 mL dispase/g tissue ⌘	• Uriel	[43–46,65]
Porcine *(Dermis)*	• 0.25% trypsin • 70% ethanol • 3% H_2O_2 • 1% Triton X-100 in 0.26% EDTA/0.69% Tris • 0.1% peracetic acid/4% ethanol	• Freytes • 72 h	[23,114–116]

(*continued on next page*)

Table 1 (*continued*)

Source Tissue	Decellularization Reagents	Solubilization Protocol	Ref.
Small Intestine			
Porcine (*Submucosa/muscularis mucosa/stratum compactum/ lamina propria*)	*Mechanical delamination of other tissue layers only*	• Voytik-Harbin • Additional step: centrifuged, dialyzed against 0.01 M acetic acid	[16,34]
Porcine (*Submucosa/muscularis mucosa/stratum compactum*)	• 0.1% peracetic acid/4% ethanol	• Freytes • 72 h	[26,56,90,101]
	• 0.1% peracetic acid/4% ethanol	• Freytes • 0.5 mg/mL pepsin	[53]
	• 0.1% peracetic acid/4% ethanol	• Freytes • 24 h	[51]
Tendon			
Human (*Flexor digitorum profudus, flexor digitorum superficialis, flexor pollicic longus*)	• 0.1% EDTA • 0.1% SDS in 0.1% EDTA	• Freytes • 0.02 M HCl • 24 h	[59,84]
Tooth			
Human (*Dentin*)	• 10% HCl • 0.5% pen/strep • 0.5 M HCl • 0.05% trypsin/0.025% EDTA	• Freytes • 84 h	[96]
Umbilical Cord			
Human	• 1% SDS and 0.5% pen/step • 0.001% Triton X-100 • 40 U/mL DNase and 1 U/mL RNase in 10 mM NaCl, 1 mM $CaCl_2$ 6 mM $MgCl_2$, and 40 mM HCl • 1% SDS and 0.5% pen/strep • 0.001% Triton X-100	• Freytes • 0.1 M HCl	[63]
Urinary Bladder			
Porcine (*Basement membrane/lamina propria*)	• 0.1% peracetic acid/4% ethanol	• Freytes	[20–24,54,56,82,91,93,99,101,116]

Freytes:

- 1 mg/mL pepsin in 0.01 M HCl
- Stir plate, RT, 48 h
- Neutralized to pH 7.4 and physiological salt with NaOH and 10x PBS

Uriel:

- High salt buffer solution (0.05 M Tris pH 7.4, 3.4 M sodium chloride, 4 mM of ethylenediaminete- traacetic acid, and 2 mM of N-ethylmaleimide) containing protease inhibitors (0.001 mg/mL pepstatin, 0.01 mg/mL aprotonin, 0.001 mg/mL leupeptin, 2 mM sodium orthova-nadate, and 1 mM phenylmethylsulfonyl fluoride)
- Homogenized with mortar and pestle
- 2 M urea buffer

Voytik-Harbin:

- 2 mg pepsin per 100 mg ECM in 0.5 M acetic acid
- 4 °C, 72 h
- Neutralized to pH 7.4 and physiological salt with NaOH and 10x PBS

Key

- ⌘ Was not lyophilized/powdered prior to solubilization
- RT – room temperature

portion (up to 99%) of acid-insoluble collagen [37,38]. Pepsin cleaves the telopeptide bonds of the collagen triple helix structure to unravel collagen fibril aggregates [39]. The ECM material is first powdered and stirred in pepsin with dilute hydrochloric acid over 48 h, as reported by Freytes et al. and designated herein as the "Freytes method" [20]. Another method involves the use of 0.5 M acetic acid instead of 0.1 M HCl as a base medium for the pepsin enzyme ("Voytik-Harbin method") [16]. Pepsin digestion or solubilization is complete when the liquid is homogenous with no visible particles [20]. Different digestion times will produce a different profile of cryptic molecules, some of which possess bioactive properties [31,40], suggesting the preferred digestion period will need to be tailored for each clinical application; times of 24–96 h have been reported (Table 1). The "solubilized ECM" or "ECM digest" forms a gel when the liquid is neutralized to physiologic pH, salt concentration ("ECM pre-gel") and temperature *in vitro* ("ECM hydrogel") in an entropy-driven process dominated by collagen kinetics. Specifically, there is an increase in entropy when collagen monomers lose water, form aggregates, and bury surface-exposed hydrophobic residues within the fibril *in vitro,* in a self-assembly process [39,41]. In practice, the "solubilized ECM" is neutralized to physiologic pH and salt concentration and kept at a low temperature well-below 37 °C, until the application of interest is identified for temperature-controlled gelation; e.g., injected by needle or catheter to gel in situ, or placed in an incubator for 3D cell culture.

Johnson et al. investigated the effect of changing a single neutralization parameter (pH, temperature, ionic strength) from standard conditions (pH 7.4, 37 °C, 1x PBS) on the material properties of an ECM hydrogel, specifically myocardial ECM hydrogel [42]. In brief, the gelation time could be modulated from $\sim$20 min at decreased salt concentration (0.5x PBS) or to >8 h at increased salt concentration (1.5x PBS). Increasing the salt concentration also decreased the storage modulus by $\sim$2–3-fold. Interestingly, lowering the gelation temperature below 22 °C was shown to inhibit gelation unlike pure collagen hydrogels that can gel between 4 and 37 °C. The impact of gelation parameters on material properties underscores the importance of understanding ECM hydrogel structure-function relationships.

Alternative methods for ECM digestion include an extraction process to solubilize and form an ECM hydrogel from soft tissue [43,44]. Proteins and glycoproteins can be extracted using a homogenization process involving pestle and mortar or high speed shear mixed within a high salt buffer that physically disrupts the ECM particles and collagen fiber structure at physiologic pH [43–47]. Homogenization involves a dispase enzymatic step that cleaves fibronectin, collagen IV, and collagen I and digests the ECM, a urea extraction step which further disrupts the non-covalent bonding and increases the solubility of the ECM proteins, and centrifugation that removes any residual non-soluble ECM components. The resulting solubilized extracts form an ECM hydrogel when increasing the temperature of the extract to 37 °C or by decreasing the pH with acetic acid to pH 4.0 ("Uriel method") [43]. The Uriel method is based on the technique established to isolate commercial products Matrigel, Myogel, and Cartigel [44]. Basement membrane complexes are believed to be formed by cells secreting a certain threshold of basement proteins at 37 °C or by decreasing the local pH at the cell surface to trigger laminin-111 arrangement; although the exact mechanism or combination thereof of pH and temperature gelation has yet to be determined [44].

While collagen kinetics and basement membrane assembly have been used to describe ECM hydrogel formation *in vitro*, the other components of the complex ECM unavoidably influence the hydrogel formation process. Brightman et al. showed that ECM hydrogels have distinct matrix assembly kinetics, fiber networks, and fibril morphology compared to purified collagen I hydrogels [34]. Addition of GAGs (heparin) or proteoglycans (decorin) to purified collagen I hydrogel show that the heparin moiety causes the collagen to gel faster and form larger fibers that are less tightly packed, while addition of decorin causes the collagen to gel faster but does not affect fibril network. The results are consistent with the known role of heparin as a nucleation site for collagen fibrillogenesis and for decorin as a known regulator of fibril self-assembly [34,39]. In addition to heparin and decorin, many other ECM proteins are known to contribute to collagen polymerization: fibronectin is known to organize collagen fibers, and minor collagens (collagen V and XI) are nucleation sites that must be present for collagen fibrillogenesis *in vivo* [48]. The Brightman et al. study [34] shows ECM glycoproteins and proteoglycans play a dynamic role in regulation of ECM hydrogel fibrillogenesis, and therefore the importance of preserving the ECM proteins in their stoichiometric ratios from the native tissues during the decellularization and solubilization steps (Table 1).

3. ECM hydrogel characterization

Source tissue type and subsequent processing steps affect the topological, biochemical, mechanical, and biological properties of an ECM hydrogel. These properties have been well characterized for SIS and UBM hydrogels, as well as many different tissue-derived hydrogels. Fig. 1 provides an overview of methods that have been used for various tissue types and is a general guide to the state of the field. Fig. 1 is not a comprehensive list since hydrogels made from various species, tissues, concentrations and processing methods have been classified only by the source tissue.

There are certain characteristics of ECM hydrogels that are widely conserved regardless of source tissue; however, some properties vary markedly and are influenced by many factors, including source tissue, source species, ECM concentration, ECM processing method, method of sterilization, and even natural variability among biologic samples.

3.1. Biochemical composition

The ECM is composed of a complex mixture of both structural and functional molecules that can be largely retained following the decellularization and solubilization processes if appropriate methods are used. However, the enzymatic solubilization process undoubtedly alters the proteins within the ECM hydrogel. Pouliot et al. directly compared the protein profile of lung ECM powder and pepsin digested lung ECM pre-gel with SDS-PAGE [49]. The protein profile shows a smear of smaller proteins in the pre-gel solution, which must be due to fragmentation of larger proteins by the enzyme since there is no extraction or purification step involved in the pepsin-based solubilization process. The extent to which this protein fragmentation affects the bioactivity of ECM hydrogels is currently unknown.

Even so, the biochemical composition of the hydrogel forms of SIS [34] and UBM [20,23] are similar to that of the intact bioscaffolds with respect to collagen and sulfated GAG (sGAG) content. Intact SIS scaffolds are composed mainly of collagen I with lesser amounts of collagens III, IV, V, and VI [17]. SIS hydrogels are known to at least contain collagens I, III, and IV and sGAGs [34]. Gel electrophoresis of UBM hydrogels shows similar bands to SIS hydrogels and both show additional bands corresponding to other ECM proteins [20]. Intact growth factors have also been confirmed in adipose [50], colon [51], liver [52], and SIS [53] ECM hydrogels, although present in reduced amounts compared to native tissue or ECM scaffolds. The impact of solubilization on cryptic peptide

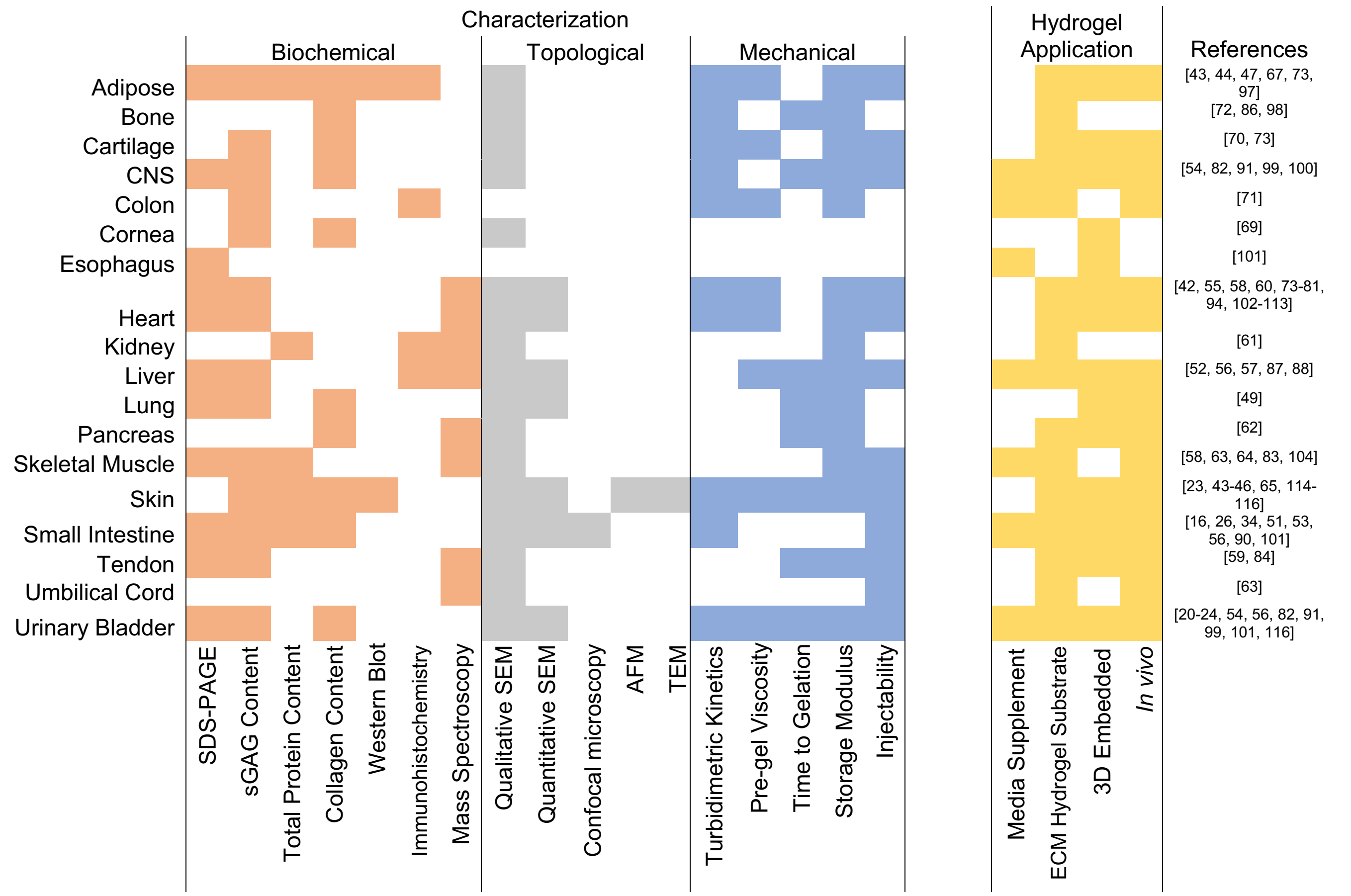

Fig. 1. Overview of techniques used to characterize and to evaluate the cellular response to ECM hydrogels thus far. ECM hydrogels derived from various species, concentrations and processing methods are categorized only by source tissue.

and matrix-bound nanovesicle content or activity has yet to be evaluated.

In spite of the similarities, the composition of the ECM is distinctive for each tissue and organ. For example, the soluble collagen content of brain ECM is significantly less than UBM and spinal cord ECM [54], but that of dermis is significantly greater than UBM [23]. Both spinal cord and dermal ECM have lower sGAG content than UBM [54]. Species-specific differences in the composition of the same tissue type ECM, such as pericardium [55] and liver [56], have also been shown.

A commonly used technique to characterize the biochemical composition of ECM hydrogels is mass spectroscopy. Reverse phase high-performance liquid chromatography interfaced with tandem mass spectroscopy (LC-MS/MS) was used to determine the proteomic profile of pepsin-solubilized hydrogels by comparing the generated protein fragments to a protein data bank. Thus far, LC-MS/MS has been used to characterize liver [57], skeletal muscle [58], tendon [59], heart [55,58,60], kidney [61], pancreas [62] and umbilical cord [63] ECM hydrogels.

3.2. Gel ultrastructure

The native ECM structure is comprised of a 3D network of fibers with both tightly and loosely associated proteoglycans and GAGs. Fiber diameter, pore size, and fiber orientation can all influence cell behavior [44]. During the decellularization and solubilization processes, the collagen fiber structure is disrupted, resulting in loss of the native fiber network. The collagen monomers self-assemble into a fibrillar network which does not exist in the pre-gel solution [64]. Scanning electron microscopy (SEM) is the most common method of visualizing the topology of hydrogels, but transmission electron microscopy (TEM) [44], atomic force microscopy (AFM) [65], and confocal microscopy [34] have also been used. SEM images of fully-formed ECM hydrogels generally show a loosely organized nanofibrous scaffold with interconnecting pores [20]. The nano-scale topography provides a high surface area to volume ratio that allows increased area for integrin binding, and is small enough to be sensed and manipulated by infiltrating cells [42,60]. An algorithm has been developed to perform automated and high-throughput analysis of SEM images with quantification of fiber diameter, pore size, and fiber alignment of hydrogels [23,56,66]. UBM hydrogels show an average fiber diameter of 74 nm [23]. Various source tissue ECMs showing an average fiber diameter of approximately 100 nm have been reported (e.g. cardiac [42], SIS [53], adipose [67]).

As stated earlier, ECM hydrogels share many common features, but the tissue of origin, processing methods, and protein concentration of the hydrogel all influence the structure of these materials. For example, pore size and fiber diameter are independent of concentration in UBM [23] and liver ECM gels [56], but vary with ECM concentration in dermal ECM gels [23]. UBM hydrogels also show randomly organized fibers, whereas more aligned fiber architecture has been observed in SIS hydrogels [53]. Qualitative analysis of SEM images show easily recognizable differences in structure depending upon the gelation mechanism (temperature- vs. pH-induced) used to create dermal hydrogels [44]. Variation in structure with species source has also been reported for liver hydrogels derived from human, rat, dog and pig [56].

Some structural characteristics of the native ECM are retained in ECM hydrogels. For example the pore size, fiber diameter and primarily flocculent fiber structure of dermal ECM hydrogels are comparable to the native basement membrane [44]. Additionally, periodic striations characteristic of the D-band morphology of native collagen can be seen in fiber networks of liver [57] and tendon [59] hydrogels.

3.3. Viscoelastic properties

Low viscosity of the pre-gel solution and application-appropriate gelation kinetics are important criteria for minimally invasive delivery. Stated differently, sufficient time is required for delivery of the pre-gel to selected anatomic sites before gelation is complete. Substrate stiffness is also known to direct stem cell differentiation and function in *in vitro* culture and also influences the remodeling outcome *in vivo* [68]. Therefore, use of an ECM hydrogel intended to define the microenvironment for stem cell delivery or recruitment can be dependent upon pre-determined hydrogel properties. Furthermore, all three of these properties (i.e. pre-gel viscosity, gelation kinetics and gel stiffness) can affect whether the injected gel is retained within the defect site or instead diffuses into the surrounding host tissue [21,22]. Turbidimetric gelation kinetics and rheology are the primary methods used to assess the viscoelastic properties of ECM hydrogels. Other methods, such as indentation [69] and compression [46,64,70] testing, AFM [65], and macroscopic rigidity [20,23,71] have been explored but will not be further reviewed herein.

The turbidimetric gelation kinetics of UBM show a sigmoidal shape similar to that of purified collagen I gels [20]. Sigmoidal gelation behavior is also observed with bone [72], cartilage [70] and spinal cord ECM [54] hydrogels, whereas brain ECM hydrogels [54] show exponential behavior. The lag phase (t_{lag}) and the time to reach half of the final turbidity ($t_{1/2}$) is greater in UBM than collagen I gels, ostensibly due to the presence of GAGs and other molecules that may modulate self-assembly [20]. The t_{lag} and $t_{1/2}$ vary with gelation mechanism [43,44] and concentration [23,71] in some cases, and are concentration-independent in others [70].

Rheology is typically utilized to determine the storage modulus, or stiffness, of the hydrogel following gelation, but can also provide the pre-gel viscosity and time to gelation. ECM pre-gel solutions show low viscosity that increases with protein concentration of the pre-gel [20,22,71]. Shear thinning behavior is also a common feature of ECM hydrogels, characterized by a decrease in the steady shear viscosity of the pre-gel with increasing shear rate [73]. This characteristic may be desirable for ECM pre-gels intended for delivery through a catheter or syringe.

Upon increasing the temperature from storage of the pre-gel at 4 °C to 37 °C, gelation of the ECM pre-gel is initiated and the resulting change in properties can be measured. The rate of gelation is greater with increasing concentration in UBM [23], bone [72], liver [57] and dermal [23] ECM hydrogels. The gelation time determined by rheology is also shorter than that determined by turbidimetric methods [20]. The final storage modulus is related to the stiffness,

Table 2
Viscoelastic properties of porcine-derived ECM hydrogels. Italicized values were estimated from representative images. Steady shear viscosities refer to the pre-gel solution. "Pre-formed" indicates that gelation was induced in an incubator at 37 °C prior to rheologic testing. * indicates time to 50% gelation. "NR" indicates "not recorded."

Tissue	Conc. (mg/mL)	Protocol (strain, frequency)	G′ (Pa)	Steady Shear Viscosity (Pa*s)	Gelation time (min)	Ref
Brain	4	5%, 1 rad/s	20.3		34.8	[54]
	6	5%, 1 rad/s	49.9		2.4	[54]
	8	5%, 1 rad/s	61.8		8.3	[54]
Cartilage	30	2%, 1 rad/s	*4000*	*3*		[73]
Colon	4	0.5%, 1 rad/s	*9*	*0.75*		[71]
	8	0.5%, 1 rad/s	*50*	*1.7*		[71]
Heart	6	2.5%, 0.4 rad/s	11.3	Pre-formed		[80]
		2.5%, 1 rad/s	6.5	Pre-formed		[78]
		NR, 1 rad/s,	5.28	Pre-formed		[42]
		NR, 6.28 rad/s	6.08	Pre-formed		[60]
	8	2.5%, 0.5 rad/s	5.3	Pre-formed		[74]
		NR, 1 rad/s,	9.52	Pre-formed		[42]
	30	2%, 1 rad/s	*800*	*33*		[73]
Liver	8	0.5%, 1 rad/s	*630*	*4.25*	*8.5*	[56]
Lung	4	0.5%, 6.28 rad/s	15.3			[49]
	6	0.5%, 6.28 rad/s	32.0			[49]
	8	0.5%, 6.28 rad/s	59.0			[49]
Pancreas	16.7	2.5%, 1 rad/s	*190*		*4.5*	[62]
Skeletal Muscle	6	NR, 1 rad/s	6.5	Pre-formed		[83]
Skin	4	0.5%, 1 rad/s	*110*	*2*		[23]
	6	0.5%, 1 rad/s	*200*	*2*		[23]
	8	0.5%, 1 rad/s	466	*7*		[23]
Spinal cord	4	5%, 1 rad/s	138		11.7	[54]
	6	5%, 1 rad/s	235		7	[54]
	8	0.5%, 1 rad/s	757		28.9	[54]
Urinary Bladder	3	5%, 1 rad/s	*6*		*10*	[20]
	4	0.5%, 1 rad/s	*110*	*0.06*		[23]
			76.6	0.084	3.2*	[22]
		5%, 1 rad/s	11.4		52.5	[54]
	6	0.5%, 1 rad/s	*40*	*0.9*		[23]
		5%, 1 rad/s	*26*		*10*	[20]
			72.8		8.47	[54]
	8	0.5%, 1 rad/s	182	*0.9*		[23]
			460	0.443	3.0*	[22]
		5%, 1 rad/s	143		19.8	[54]

and solid-like behavior of the gel is confirmed when the storage modulus is greater than the loss modulus by approximately one order of magnitude, and the storage modulus is largely independent of frequency [20]. An increase in storage modulus occurs with increasing protein concentration for multiple source tissues including UBM [20,22,23], lung [49], heart [42], bone [72], colon [71], and liver [57]. Frequency sweep analysis after gelation shows very little frequency dependence of the storage modulus, indicative of a stable and uniform gel [22,23,57].

A substantial strain-dependence is observed in some ECM hydrogels, with an increase in modulus occurring with increased strain [49,72] and an irreversible change in modulus above 5% [49]. The storage modulus of hydrogels has been determined for gels formed directly on the rheometer, and for gels pre-formed in an incubator as long as 24 h prior to rheological testing. The influence of strain and gelation method on observed modulus has yet to be studied, but the large variations could be partially due to different testing methods used by each group [49].

Table 2 shows the concentration, testing parameters, and final storage modulus of porcine-derived ECM hydrogels. The pre-gel steady shear viscosity and time to gelation as determined by rheology are included where available. The dependence of storage modulus on source tissue, concentration, testing parameters and natural variability between samples is evident. The storage modulus of the ECM hydrogel is frequently lower than the respective tissue from which the hydrogel is derived. The hydrogel should be thought of, at least in part, as an inductive template to recruit cells that will secrete *de novo* ECM comprising the stiffness of the new tissue. Though ECM hydrogels derived only from porcine tissues are included in this table, species-dependence of viscoelastic properties has also been noted [56].

Another important ECM hydrogel design criterion is injectability. While injectability may be related to the viscoelastic properties (ECM pre-gel viscosity and gelation time), injectability has been independently confirmed *in vitro* and/or *in vivo* for heart [55,60,74–81], spinal cord [82], small intestine [26,51], umbilical cord [63], skeletal muscle [63,64,83], tendon [59,84], dermal [23], lung [49], liver [57], cartilage [70], urinary bladder [21,22,24,82] and adipose [50,67] ECM hydrogels with reported 18–27 gauge syringes or catheters. For example, porcine myocardial gel (6 mg/mL) was confirmed to be injectable through a 27 gauge catheter [75], and then confirmed to be injectable via NOGA guided MyoSTAR catheter (27 gauge), which is the current gold standard delivery device used in cellular cardiomyoplasty procedures [75]. The material remained injectable for 1 h at room temperature during injection, a clear advantage compared to other natural materials such as collagen and fibrin that gel too quickly and cannot be delivered by catheter [75].

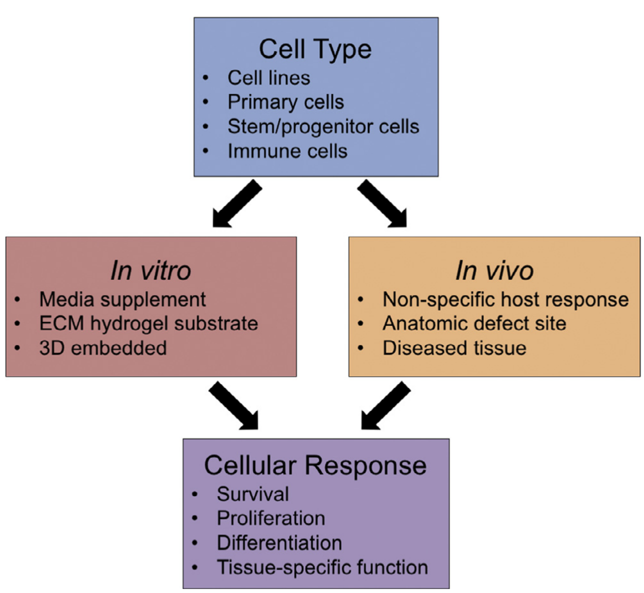

Fig. 2. General approaches to assess cellular response to ECM hydrogels. The response of various cell types *in vitro* or *in vivo* can be evaluated.

4. Cellular response to ECM hydrogels

The ECM represents, in large part, the microenvironmental niche of every cell. The mechanism by which the native ECM influences cell behavior likely includes the physical and mechanical properties of the ECM, embedded cytokines and chemokines, cryptic peptides formed during ECM remodeling, and matrix-bound nanovesicle mediated events, among others. The signaling mechanisms that are preserved during production of an ECM hydrogel from a source tissue are only partially understood and will obviously influence cell viability, proliferation, migration, morphology, differentiation and phenotype. Established methods to evaluate the cellular response to ECM hydrogels both *in vitro* and *in vivo* are summarized in Fig. 2.

The viability of cells cultured on the surface of ECM hydrogels *in vitro* has been consistently shown for cell lines [23,54,63,64,70,71,83], primary cells [57,63,69,71,75,83,85], and stem cells [44,49,50,73,82,86]. In addition, the innate bioactivity of soluble factors within the ECM has been demonstrated using *in vitro* culture with media supplemented with solubilized ECM to remove the influence of hydrogel structure on the function of cells.

Wolf et al. studied the response of 3T3 fibroblasts and C2C12 myoblast cells to UBM and dermal ECM hydrogels by three different methods: cells seeded on the surface of pre-formed gels (ECM hydrogel substrate), cells embedded within gels (3D embedded), and gel placement in an anatomic defect site *in vivo* [23]. Almost 100% viability of 3T3 fibroblasts and C2C12 myoblasts was observed after 7 days of culture for all configurations investigated *in vitro*. C2C12 myoblast cells seeded on the surface of the dermal ECM hydrogels fused into large diameter, multinucleated myotubes with radial alignment, whereas cells cultured on the surface or embedded within UBM and embedded within dermal ECM formed smaller elongated cell structures. Implantation of the hydrogels within a rodent partial thickness abdominal wall defect produced a significantly greater area of *de novo* muscle formation when the defects were treated with UBM hydrogel compared to unrepaired defects. This result likely represents the combination of microstructure, mechanical properties, and bioactivity. The collagen fiber ultrastructure and low storage modulus of UBM hydrogels allows for cell infiltration and fibroblast mediated contraction of the gel, two important aspects of wound healing [23].

4.1. Comparison to collagen and/or Matrigel

Cell behavior in response to ECM hydrogels has consistently been shown to be comparable to Matrigel and/or collagen substrate for liver [87,88], skeletal muscle [58], heart [58] and fat [43–45,47,67] applications. Uriel et al. [43] showed that primary rat pre-adipocytes cultured on the surface of adipose ECM hydrogels (1 mg/mL) formed colonies that were significantly larger compared to Matrigel (1 mg/mL) after 7 days indicative of enhanced pre-adipocyte differentiation. Furthermore, the adipose ECM hydrogels (1 mg/mL) that were formed by reducing pH to 4.0 showed significantly greater adipose area compared to Matrigel (1 mg/mL) at 1, 3, and 6 weeks *in vivo* in an epigastric pedicle model.

5. *In vivo* applications of ECM hydrogels

Structure-function relationships of ECM hydrogels can provide a basis for predicting the appropriate hydrogel formulation for given applications. Although *in vitro* structure-function relationships are important to understand, their relationship to *in vivo* applications are largely unknown. There have been limited experiments with ECM hydrogels in two anatomic locations: the heart and the brain.

5.1. Heart

Cardiac-derived gels are being investigated for cardiac reconstruction following ischemic injury [42,55,58,60,75–78,81]. Heterologous ECM hydrogels have been evaluated in the heart but formed cartilaginous tissue suggesting that tissue-specific cues may be necessary for appropriate cardiac tissue remodeling [75]. The Christman laboratory has investigated different cardiac tissue types for cardiac application including 1) the effect of species (porcine versus human) [60], and 2) the effect of pericardium versus myocardium [55].

Both porcine and human source tissue has been evaluated for clinical translation. Porcine cardiac tissue is more homogeneous for variables such as diet, age, and strain unlike human cadaveric donor heart tissue which involves a range of ages, disease states, and co-morbidities [60,76]. Alternatively, a human ECM source tissue has been cited as mitigating the risk for xenogeneic disease transfer [60], although there has not been a reported case of zoonotic disease in the millions of patients that have received porcine ECM scaffolds or porcine tissue (e.g., porcine heart valves) to date [89]. Both porcine and human myocardial ECM formed similar hydrogel ultrastructure *in vivo* after injection into the rat left ventricular myocardium [60]. However, perhaps most importantly, over half of the human myocardial pre-gel solutions did not form gels even allowing for the same DNA and lipid content. The differences may be attributed to the requirement for a "more harsh" decellularization protocol (e.g., longer SDS incubation, lipid/DNA removal steps) required as a result of the increased ECM crosslinking and adipose tissue of the human tissue (donor age of human tissue ranged from 41–69 years). Johnson et al. eventually recommended porcine myocardial ECM hydrogel as the preferred source for clinical translation over human myocardial ECM hydrogel because of the increased tissue availability, relatively more gentle decellularization protocol, and more reliable gelation [60]. Human tissue was recommended as a useful model system for *in vitro* study of the role of human ECM in cardiac disease.

Two different tissue types within the heart were evaluated for myocardial repair. The pericardium is the fibrous sac surrounding the heart primarily composed of compact collagen and elastin fibers. While not tissue specific, the pericardium was explored as a potentially autologous therapy because the pericardium can be resected from the heart without adverse effect on heart function and is currently FDA approved for structural reinforcement in other body applications. The pericardial ECM hydrogel (6.6 mg/mL) and myocardial ECM hydrogel (6 mg/mL) were evaluated in the non-diseased, orthotopic location, and injected into the rat LV wall in separate studies. Both pericardial ECM and myocardial ECM hydrogels supported vascular cell infiltration (endothelial cells, smooth muscle cells) and almost identical arteriole formation within 2 weeks (51 ± 42 vessels/mm^2, 52 ± 20 arterioles/mm^2 respectively) [55,75]. In conclusion, it was suggested that pericardial ECM may be a candidate for same-patient ECM sourcing [55,76], but myocardial ECM hydrogel was preferred for preclinical studies in the rat and pig.

Porcine myocardial ECM hydrogel has been evaluated in both small and large animal models of myocardial infarction (MI). The *in vivo* pathogenic microenvironment poses unique challenges such as the sustained release of pro-inflammatory cytokines thought to promote cell apoptosis or necrosis, matrix metalloproteinase (MMP) production that degrades the matrix, and an ischemic/hypoxic microenvironment. Myocardial ECM preserved cardiac function in a rat model of MI while the saline treated rats worsened 4 weeks after injection compared to baseline 1 week prior to injection. Specifically, myocardial ECM showed an increased ejection fraction (EF) and a relatively decreased percent change in end-systolic volume (ESV) and end-diastolic volume (EDV) compared to saline treated control; however, none of the three markers were significantly different compared to controls [79]. In an established large animal model, the myocardial ECM was delivered by the clinical standard transendocardial catheter two weeks after MI. After three months, myocardial ECM treated groups showed significant improvement in three measures of cardiac function: 1) echocardiography, 2) global wall motion index scoring, and 3) electromechanical NOGA mapping [77]. Corroborating the functional improvement, myocardial ECM treated animals promoted healthy muscle and blood vessel formation in infarcted areas: a distinct band of muscle that stained positive for troponin T below the endocardium was present in the myocardial ECM treated groups, and the muscle was significantly larger than control muscle. The myocardial ECM treated group showed significantly reduced fibrosis and neovascularization foci below the endocardium compared to controls.

Recently, Wassenaar et al. investigated the molecular mechanisms underlying the ability of myocardial ECM to mitigate negative LV remodeling using whole transcriptome analysis in the rat model of MI [81]. This was the first study to determine global gene expression changes with ECM hydrogel treatment. The myocardial ECM compared to saline control after 1 week of treatment showed several significantly altered pathways at the tissue level including: altered inflammatory response; decreased cardiomyocyte apoptosis, altered myocardial metabolism, enhanced blood vessel development, increased cardiac transcription factor expression, and increased progenitor cell recruitment. Angiogenesis is one of the processes modulated by ECM hydrogel treatment and a critically important process relevant to other *in vivo* applications. Wassenaar et al. speculate the ECM hydrogel may directly recruit endothelial progenitor cells through pro-angiogenic growth factors or matricryptic peptides, provide a scaffold for blood vessel formation, or modulate the recruited macrophages' secretory profile [81].

5.2. Brain

While the use of homologous ECM has been investigated for cardiac applications, the use of heterologous ECM, specifically UBM hydrogel, has been evaluated in brain applications to treat traumatic brain injury (TBI) [24] and stroke [21,22].

In a rat model of TBI [24], UBM hydrogel (5 mg/mL) was delivered one day after controlled cortical impact injury. UBM mitigated adverse tissue damage with decreased lesion volume, decreased white matter injury, and increased vestibulomotor function at 21 days. However, no cognitive improvement was shown by the Morris water maze task. While the UBM hydrogel showed functional improvement in tissue repair, it has yet to show the "holy grail" of cognitive improvement. It was suggested the brain may be a type of clinical application which requires the addition of neural stem cells to the ECM hydrogel, or other tailoring of ECM hydrogel properties.

ECM concentration-specific properties of UBM hydrogels were also used to selectively affect the material retention [22] and the immune cell infiltrate [21] in a small animal model of chronic stroke. Specifically, UBM hydrogel (1–8 mg/mL) was delivered

14 days after middle cerebral artery occlusion in the rat. UBM hydrogels <3 mg/mL did not form a gel within the stroke lesion and instead diffused into the surrounding brain tissue as early as 24 h, the earliest time point investigated [22]. In a follow-up study, it was shown that with the use of UBM hydrogels <3 mg/mL, the cells did not have a medium through which to infiltrate the lesion and instead accumulated around the lesion site [21]. UBM hydrogels >3 mg/mL formed a hydrogel within the stroke cavity that interfaced with the adjacent tissue [21,22]. Because a distinct host/tissue interface was formed, >3 mg/mL treatment also showed extensive cell infiltration 1 day after delivery [21]. Macrophages and microglia were accompanied by neural progenitor cells, endothelial cells, oligodendrocytes, and astrocytes. An understanding of the cell infiltrate based upon the viscoelastic properties of the hydrogel in the brain is crucial since these cells will ultimately remodel the ECM and replace it with *de novo* matrix. While this application would suggest that the >3 mg/mL UBM hydrogels would be preferred, other tissue applications may show improved outcomes if ECM signaling molecules would be released and permeate the surrounding tissue.

For ECM hydrogels >3 mg/mL that may be retained within the lesion and allow for immune cell infiltration, there are several concentration-dependent properties that may be important in the context of clinical delivery [22]. Four and 8 mg/mL UBM hydrogels were tested *in vitro* as candidates for brain repair after stroke injury. Both 4 and 8 mg/mL hydrogels showed ideal properties of an injectable therapy: viscosities ranging from that of water to honey (0.084 Pa*s and 0.443 Pa*s respectively), stably formed gels ($G' > G''$ by ~10-fold), and 50% gelation times (~3 min) considered to be a reasonable time frame in the operating room. The storage moduli or "stiffness" differed more dramatically for the 4 and 8 mg/mL hydrogel, at 76 and 460 Pa respectively. Brain tissue storage moduli has been reported between 200 and 500 Pa as a target moduli range [22], however it is important to state again the recruited cells will ultimately remodel the matrix.

5.3. Safety

The *in vivo* safety of an ECM hydrogel for any clinical application is obviously an important consideration. ECM hydrogels were considered safe in the aforementioned heart and brain *in vivo* applications. The ECM treated MI induced pigs did not show arrhythmias, thromboembolism or ischemia 3 months after myocardial ECM injection [77]. Hemocompatibility was further corroborated *in vitro* when the myocardial ECM gels were tested at a physiologically relevant concentration and shown not to accelerate coagulation.

Zhang et al. also showed that the UBM hydrogel (5 mg/mL) did not have a deleterious effect when injected into the normal brain [24]. There was no reactive astrocytosis (GFAP+), and no neuronal degeneration at 1, 3, and 7 days after UBM hydrogel injection. Microglial activation and degenerate neurons were shown at 1 and 3 days along the needle track and injection site, but was no different than PBS control; and was resolved by 21 days.

The potential unintended presence of ECM hydrogels in peripheral organs was evaluated in the studies of myocardial injection, and would be a safety concern relevant to all ECM hydrogel applications. Myocardial ECM hydrogels were not found at 2 h in the pig lung, liver, spleen, kidney and brain [79], nor at 3 months [77]. Each clinical application of ECM hydrogels would likely have a distinctive profile of safety measures.

5.4. In vivo host response

The clinical applications of ECM involving the heart and brain did not elicit an adverse immune response. In general, ECM hydrogels have been well-tolerated in a wide variety of *in vivo* applications. No adverse immune response was shown after ECM hydrogels were injected in the heart [55,60,75–81], fat [43,45,47,50,67], liver [57], brain [21,22,24] skeletal muscle [23,63,64,83], tendon [26,59,84], spinal cord [82], lung [49], cartilage [70], or colon [51,71], and these studies included both homologous and heterologous ECM hydrogels. The findings *in vivo* are consistent with *in vitro* studies that have shown the pepsin-digested ECM ("pre-gel") promotes a regulatory ("M2-like") macrophage activation state, which is associated with a constructive remodeling response *in vivo* [71,90,91]. For example, macrophages activated toward an M2-like phenotype with solubilized ECM promoted downstream effects such as stimulating the migration and myogenesis of skeletal muscle progenitor cells [90]. In SIS hydrogel treatment of ulcerative colitis *in vivo*, the ECM modulated the macrophage response towards a predominately regulatory state by decreasing the number of pro-inflammatory ("M1-like") activated macrophages, as opposed to increasing the number of M2-like macrophages [71]. This effect of altering the innate immune response by shifting the M2:M1 ratio is observed in the host response to solid ECM scaffolds as well [90].

5.5. Summary of in vivo applications

Heart and brain were selected as two organ systems with a need for a minimally invasive, injectable therapy. The heart showed safety and efficacy of myocardial ECM hydrogel in small and large animal model of disease up to 3 months, and is currently being evaluated in a Phase I clinical trial (ClinicalTrial.gov Identifier: NCT02305602) [92]. The brain case study showed the importance of investigating multiple ECM concentrations to determine preferred characteristics of an injectable therapy for central nervous system (CNS) applications, including delivery, facilitation of the immune cell infiltrate, and mitigation of the default response to injury. Future work in the brain will likely identify the balance of factors required for cognitive improvement. Overall, each new therapeutic application will need a thorough understanding of the ECM hydrogel structure-function relationships for successful clinical translation. Relevant references to other organ *in vivo* applications can be found in Fig. 1.

6. Future perspectives

With more than 70 papers published in the last decade it is evident that the therapeutic potential of ECM hydrogels is recognized. Characterization of hydrogel structure and function *in vitro* have provided a basis for selection of appropriate source tissue and hydrogel formulation in selected body systems. However, the relationship between *in vitro* structure-function and *in vivo* application is still largely unknown for most other clinical applications.

The mechanisms by which ECM hydrogels mediate cell behavior are not fully understood. Several hypotheses have been suggested including the possibility that the architecture of the gelled hydrogel comprises a pore size and fiber diameter suitable for endogenous cell infiltration [93]. Additionally, the bioinductive hydrogel provides tissue-specific cues, likely through the release of bound growth factors [27], or the creation of cryptic peptides or the exposure of bioactive motifs [29–32]. The recent report of bioactive matrix-bound nanovesicles within biologic scaffolds [33] provides a new possibility for study to determine the mechanisms contributing to the constructive tissue remodeling facilitated by ECM hydrogels.

The use of ECM hydrogels as a delivery vehicle is an obvious area for future study. Although a standalone ECM biomaterial therapy offers practical advantages by way of reduced regulatory concerns, ease of manufacturing and route to market, combinations of ECM hydrogels with growth factors and/or cells may provide significant mutual enhancement. Recent studies have shown that sulfated GAGs within ECM hydrogels bind to growth factors with prolonged release of basic fibroblast growth factor and heparin-binding growth factor that enhances therapeutic effects [78,94]. ECM hydrogels have also been used as a delivery system for growth factor containing microparticles to enhance skeletal tissue repair within an *ex vivo* chick femur defect model [95]. Cell therapy for neurological conditions may require integration with an appropriate biomaterial to support cells during transplantation and provide a structural support system post implantation. Recent investigations of ECM hydrogels for CNS applications have included the assessment of different source tissues to direct cell differentiation [96] and the transplantation of human neural stem cells embedded within ECM hydrogels to support the creation of *de novo* tissue [25]. Stem cells and primary cells have also been embedded within lung [49], liver [57], spinal cord [82], and adipose [50] ECM hydrogels to improve the tissue remodeling outcome.

In conclusion, the use of ECM hydrogels for a variety of clinical applications is in its infancy, but has shown promise. The combination of *in vitro* and *in vivo* studies designed to understand mechanical and material properties, the effects of processing methods upon hydrogel performance, the mechanisms by which such hydrogels influence cell behavior and tissue remodeling, and the safety of ECM hydrogels should advance their clinical utility.

Acknowledgements

Funding sources: LTS was supported by the National Institute of Biomedical Imaging and Bioengineering of the National Institutes of Health – United States (2T32 EB001026-11). LJW was funded by a Marie Curie International Outgoing Fellowship under REA grant agreement no. 624841.

References

[1] J.L. Drury, D.J. Mooney, Hydrogels for tissue engineering: scaffold design variables and applications, Biomaterials 24 (2003) 4337–4351.
[2] J.S. Choi, B.S. Kim, J.D. Kim, Y.C. Choi, H.Y. Lee, Y.W. Cho, In vitro cartilage tissue engineering using adipose-derived extracellular matrix scaffolds seeded with adipose-derived stem cells, Tissue Eng. Part A 18 (2012) 80–92.
[3] J.J. Mercuri, S.S. Gill, D.T. Simionescu, Novel tissue-derived biomimetic scaffold for regenerating the human nucleus pulposus, J. Biomed. Mater. Res. A 96 (2011) 422–435.
[4] J.J. Mercuri, S. Patnaik, G. Dion, S.S. Gill, J. Liao, D.T. Simionescu, Regenerative potential of decellularized porcine nucleus pulposus hydrogel scaffolds: stem cell differentiation, matrix remodeling, and biocompatibility studies, Tissue Eng. Part A 19 (2013) 952–966.
[5] E.C. Beck, M. Barragan, T.B. Libeer, S.L. Kieweg, G.L. Converse, R.A. Hopkins, C.J. Berkland, M.S. Detamore, Chondroinduction from naturally derived cartilage matrix: a comparison between devitalized and decellularized cartilage encapsulated in hydrogel pastes, Tissue Eng. Part A 22 (2016) 665–679.
[6] E.C. Beck, M. Barragan, M.H. Tadros, E.A. Kiyotake, F.M. Acosta, S.L. Kieweg, M. S. Detamore, Chondroinductive hydrogel pastes composed of naturally derived devitalized cartilage, Ann. Biomed. Eng. 44 (2016) 1863–1880.
[7] M.J. Bissell, H.G. Hall, G. Parry, How does the extracellular matrix direct gene expression?, J Theor. Biol. 99 (1982) 31–68.
[8] R.O. Hynes, The evolution of metazoan extracellular matrix, J. Cell Biol. 196 (2012) 671–679.
[9] M.W. Tibbitt, K.S. Anseth, Hydrogels as extracellular matrix mimics for 3D cell culture, Biotechnol. Bioeng. 103 (2009) 655–663.
[10] R.A. Elliott Jr., J.G. Hoehn, Use of commercial porcine skin for wound dressings, Plast. Reconstr. Surg. 52 (1973) 401–405.
[11] S.F. Badylak, G.C. Lantz, A. Coffey, L.A. Geddes, Small intestinal submucosa as a large diameter vascular graft in the dog, J. Surg. Res. 47 (1989) 74–80.
[12] G.C. Lantz, S.F. Badylak, A.C. Coffey, L.A. Geddes, W.E. Blevins, Small intestinal submucosa as a small-diameter arterial graft in the dog, J. Invest. Surg. 3 (1990) 217–227.
[13] G.C. Lantz, S.F. Badylak, A.C. Coffey, L.A. Geddes, G.E. Sandusky, Small intestinal submucosa as a superior vena cava graft in the dog, J. Surg. Res. 53 (1992) 175–181.
[14] G.E. Sandusky Jr., S.F. Badylak, R.J. Morff, W.D. Johnson, G. Lantz, Histologic findings after in vivo placement of small intestine submucosal vascular grafts and saphenous vein grafts in the carotid artery in dogs, Am. J. Pathol. 140 (1992) 317–324.
[15] G.C. Lantz, S.F. Badylak, M.C. Hiles, A.C. Coffey, L.A. Geddes, K. Kokini, G.E. Sandusky, R.J. Morff, Small intestinal submucosa as a vascular graft: a review, J. Invest. Surg. 6 (1993) 297–310.
[16] S.L. Voytik-Harbin, A.O. Brightman, Small intestinal submucosa: a tissue derived extracellular matrix that promotes tissue-specific growth and differentiation of cells in vitro, Tissue Eng. 4 (1998) 157–174.
[17] S.F. Badylak, D.O. Freytes, T.W. Gilbert, Extracellular matrix as a biological scaffold material: structure and function, Acta Biomater. 5 (2009) 1–13.
[18] T. Zantop, T.W. Gilbert, M.C. Yoder, S.F. Badylak, Extracellular matrix scaffolds are repopulated by bone marrow-derived cells in a mouse model of Achilles tendon reconstruction, J. Orthop. Res. 24 (2006) 1299–1309.
[19] T.W. Gilbert, D.B. Stolz, F. Biancaniello, A. Simmons-Byrd, S.F. Badylak, Production and characterization of ECM powder: implications for tissue engineering applications, Biomaterials 26 (2005) 1431–1435.
[20] D.O. Freytes, J. Martin, S.S. Velankar, A.S. Lee, S.F. Badylak, Preparation and rheological characterization of a gel form of the porcine urinary bladder matrix, Biomaterials 29 (2008) 1630–1637.
[21] H. Ghuman, A.R. Massensini, J. Donnelly, S.M. Kim, C.J. Medberry, S.F. Badylak, M. Modo, ECM hydrogel for the treatment of stroke: characterization of the host cell infiltrate, Biomaterials 91 (2016) 166–181.
[22] A.R. Massensini, H. Ghuman, L.T. Saldin, C.J. Medberry, T.J. Keane, F.J. Nicholls, S.S. Velankar, S.F. Badylak, M. Modo, Concentration-dependent rheological properties of ECM hydrogel for intracerebral delivery to a stroke cavity, Acta Biomater. 27 (2015) 116–130.
[23] M.T. Wolf, K.A. Daly, E.P. Brennan-Pierce, S.A. Johnson, C.A. Carruthers, A. D'Amore, S.P. Nagarkar, S.S. Velankar, S.F. Badylak, A hydrogel derived from decellularized dermal extracellular matrix, Biomaterials 33 (2012) 7028–7038.
[24] L. Zhang, F. Zhang, Z. Weng, B.N. Brown, H. Yan, X.M. Ma, P.S. Vosler, S.F. Badylak, C.E. Dixon, X.T. Cui, J. Chen, Effect of an inductive hydrogel composed of urinary bladder matrix upon functional recovery following traumatic brain injury, Tissue Eng. Part A 19 (2013) 1909–1918.
[25] E. Bible, F. Dell'Acqua, B. Solanky, A. Balducci, P.M. Crapo, S.F. Badylak, E.T. Ahrens, M. Modo, Non-invasive imaging of transplanted human neural stem cells and ECM scaffold remodeling in the stroke-damaged rat brain by (19)F- and diffusion-MRI, Biomaterials 33 (2012) 2858–2871.
[26] M.B. Fisher, R. Liang, H.J. Jung, K.E. Kim, G. Zamarra, A.J. Almarza, P.J. McMahon, S.L. Woo, Potential of healing a transected anterior cruciate ligament with genetically modified extracellular matrix bioscaffolds in a goat model, Knee Surg. Sports Traumatol. Arthrosc. 20 (2012) 1357–1365.
[27] S.F. Badylak, The extracellular matrix as a scaffold for tissue reconstruction, Semin. Cell Dev. Biol. 13 (2002) 377–383.
[28] R. Londono, S.F. Badylak, Biologic scaffolds for regenerative medicine: mechanisms of in vivo remodeling, Ann. Biomed. Eng. 43 (2015) 577–592.
[29] A. Sarikaya, R. Record, C.C. Wu, B. Tullius, S. Badylak, M. Ladisch, Antimicrobial activity associated with extracellular matrices, Tissue Eng. 8 (2002) 63–71.
[30] E.P. Brennan, J. Reing, D. Chew, J.M. Myers-Irvin, E.J. Young, S.F. Badylak, Antibacterial activity within degradation products of biological scaffolds composed of extracellular matrix, Tissue Eng. 12 (2006) 2949–2955.
[31] V. Agrawal, S. Tottey, S.A. Johnson, J.M. Freund, B.F. Siu, S.F. Badylak, Recruitment of progenitor cells by an extracellular matrix cryptic peptide in a mouse model of digit amputation, Tissue Eng. Part A 17 (2011) 2435–2443.
[32] J.E. Reing, L. Zhang, J. Myers-Irvin, K.E. Cordero, D.O. Freytes, E. Heber-Katz, K. Bedelbaeva, D. McIntosh, A. Dewilde, S.J. Braunhut, S.F. Badylak, Degradation products of extracellular matrix affect cell migration and proliferation, Tissue Eng. Part A 15 (2009) 605–614.
[33] L. Huleihel, G.S. Hussey, J.D. Naranjo, L. Zhang, J.L. Dziki, N.J. Turner, D.B. Stolz, S.F. Badylak, Matrix-bound nanovesicles within ECM bioscaffolds, Sci. Adv. 2 (2016) e1600502.
[34] A.O. Brightman, B.P. Rajwa, J.E. Sturgis, M.E. McCallister, J.P. Robinson, S.L. Voytik-Harbin, Time-lapse confocal reflection microscopy of collagen fibrillogenesis and extracellular matrix assembly in vitro, Biopolymers 54 (2000) 222–234.
[35] P.M. Crapo, T.W. Gilbert, S.F. Badylak, An overview of tissue and whole organ decellularization processes, Biomaterials 32 (2011) 3233–3243.
[36] T.J. Keane, R. Londono, N.J. Turner, S.F. Badylak, Consequences of ineffective decellularization of biologic scaffolds on the host response, Biomaterials 33 (2012) 1771–1781.
[37] M.P. Drake, P.F. Davison, S. Bump, F.O. Schmitt, Action of proteolytic enzymes on tropocollagen and insoluble collagen, Biochemistry 5 (1966) 301–312.
[38] E.J. Miller, Structural studies on cartilage collagen employing limited cleavage and solubilization with pepsin, Biochemistry 11 (1972) 4903–4909.
[39] D.J.S. Hulmes, Collagen Diversity, Synthesis, and Assembly, Springer, 2008.
[40] V. Agrawal, J. Kelly, S. Tottey, K.A. Daly, S.A. Johnson, B.F. Siu, J. Reing, S.F. Badylak, An isolated cryptic peptide influences osteogenesis and bone remodeling in an adult mammalian model of digit amputation, Tissue Eng. Part A 17 (2011) 3033–3044.
[41] J. Parkinson, K.E. Kadler, A. Brass, Simple physical model of collagen fibrillogenesis based on diffusion limited aggregation, J. Mol. Biol. 247 (1995) 823–831.

[42] T.D. Johnson, S.Y. Lin, K.L. Christman, Tailoring material properties of a nanofibrous extracellular matrix derived hydrogel, Nanotechnology 22 (2011) 494015.
[43] S. Uriel, J.J. Huang, M.L. Moya, M.E. Francis, R. Wang, S.Y. Chang, M.H. Cheng, E.M. Brey, The role of adipose protein derived hydrogels in adipogenesis, Biomaterials 29 (2008) 3712–3719.
[44] S. Uriel, E. Labay, M. Francis-Sedlak, M.L. Moya, R. Weichselbaum, N. Ervin, Z. Cankova, E.M. Brey, Extraction and assembly of tissue-derived gels for cell culture and tissue engineering, Tissue Eng. Part C (2009) 15.
[45] M.-H. Cheng, S. Uriel, M.L. Moya, M. Francis-Sedlak, R. Wang, J.-J. Huang, S.-Y. Chang, E.M. Brey, Dermis-derived hydrogels support adipogenesis *in vivo*, J. Biomed. Mater. Res., Part A 92A (2010) 852–858.
[46] S.P. Pilipchuk, M.K. Vaicik, J.C. Larson, E. Gazyakan, M.-H. Cheng, E.M. Brey, Influence of crosslinking on the stiffness and degradation of dermis-derived hydrogels, J. Biomed. Mater. Res., Part A 101 (2013) 2883–2895.
[47] C.J. Poon, E. Pereira, M.V. Cotta, S. Sinha, J.A. Palmer, A.A. Woods, W.A. Morrison, K.M. Abberton, Preparation of an adipogenic hydrogel from subcutaneous adipose tissue, Acta Biomater. 9 (2013) 5609–5620.
[48] K.E. Kadler, A. Hill, E.G. Canty-Laird, Collagen fibrillogenesis: fibronectin, integrins, and minor collagens as organizers and nucleators, Curr. Opin. Cell Biol. 20 (2008) 495–501.
[49] R.A. Pouliot, P.A. Link, N.S. Mikhaiel, M.B. Schneck, M.S. Valentine, F.J. Kamga Gninzeko, J.A. Herbert, M. Sakagami, R.L. Heise, Development and characterization of a naturally derived lung extracellular matrix hydrogel, J. Biomed. Mater. Res. A 104 (2016) 1922–1935.
[50] E.J. Kim, J.S. Choi, J.S. Kim, Y.C. Choi, Y.W. Cho, Injectable and thermosensitive soluble extracellular matrix and methylcellulose hydrogels for stem cell delivery in skin wounds, Biomacromolecules 17 (2016) 4–11.
[51] T.J. Keane, J. Dziki, E. Sobieski, A. Smoulder, A. Castleton, N.J. Turner, L.J. White, S. Badylak, Restoring mucosal barrier function and modifying macrophage phenotype with an extracellular matrix hydrogel: potential therapy for ulcerative colitis, J. Chron's Colitis (2016).
[52] K.M. Park, K.H. Hussein, S.H. Hong, C. Ahn, S.R. Yang, S.M. Park, O.K. Kweon, B. M. Kim, H.M. Woo, Decellularized liver extracellular matrix as promising tools for transplantable bioengineered liver promotes hepatic lineage commitments of induced pluripotent stem cells, Tissue Eng. Part A 22 (2016) 449–460.
[53] R. Liang, G. Yang, K.E. Kim, A. D'Amore, A.N. Pickering, C. Zhang, S.L.Y. Woo, Positive effects of an extracellular matrix hydrogel on rat anterior cruciate ligament fibroblast proliferation and collagen mRNA expression, J. Orthop. Transl. 3 (2015) 114–122.
[54] C.J. Medberry, P.M. Crapo, B.F. Siu, C.A. Carruthers, M.T. Wolf, S.P. Nagarkar, V. Agrawal, K.E. Jones, J. Kelly, S.A. Johnson, S.S. Velankar, S.C. Watkins, M. Modo, S.F. Badylak, Hydrogels derived from central nervous system extracellular matrix, Biomaterials 34 (2013) 1033–1040.
[55] S. Seif-Naraghi, M. Salvatore, P. Schup-Magoffin, D. Hu, K. Christman, Design and characterization of an injectable pericardial matrix gel: a potentially autologous scaffold for cardiac tissue engineering, Tissue Eng. Part A 16 (2010) 2017–2027.
[56] A.E. Loneker, D.M. Faulk, G.S. Hussey, A. D'Amore, S.F. Badylak, Solubilized liver extracellular matrix maintains primary rat hepatocyte phenotype in-vitro, J. Biomed. Mater. Res. A 104 (2016) 957–965.
[57] J.S. Lee, J. Shin, H.M. Park, Y.G. Kim, B.G. Kim, J.W. Oh, S.W. Cho, Liver extracellular matrix providing dual functions of two-dimensional substrate coating and three-dimensional injectable hydrogel platform for liver tissue engineering, Biomacromolecules 15 (2014) 206–218.
[58] J.A. DeQuach, V. Mezzano, A. Miglani, S. Lange, G.M. Keller, F. Sheikh, K.L. Christman, Simple and high yielding method for preparing tissue specific extracellular matrix coatings for cell culture, PLoS ONE 5 (2010) e13039.
[59] S. Farnebo, C.Y. Woon, T. Schmitt, L.M. Joubert, M. Kim, H. Pham, J. Chang, Design and characterization of an injectable tendon hydrogel: a novel scaffold for guided tissue regeneration in the musculoskeletal system, Tissue Eng. Part A 20 (2014) 1550–1561.
[60] T.D. Johnson, J.A. Dequach, R. Gaetani, J. Ungerleider, D. Elhag, V. Nigam, A. Behfar, K.L. Christman, Human versus porcine tissue sourcing for an injectable myocardial matrix hydrogel, Biomater. Sci. 2014 (2014) 60283D.
[61] R.J. Nagao, J. Xu, P. Luo, J. Xue, Y. Wang, S. Kotha, W. Zeng, X. Fu, J. Himmelfarb, Y. Zheng, Decellularized human kidney cortex hydrogels enhance kidney microvascular endothelial cell maturation and quiescence, Tissue Eng. Part A (2016).
[62] D. Chaimov, L. Baruch, S. Krishtul, I. Meivar-Levy, S. Ferber, M. Machluf, Innovative encapsulation platform based on pancreatic extracellular matrix achieve substantial insulin delivery, J. Control. Release (2016).
[63] J.L. Ungerleider, T.D. Johnson, M.J. Hernandez, D.I. Elhag, R.L. Braden, M. Dzieciatkowska, K.G. Osborn, K.C. Hansen, E. Mahmud, K.L. Christman, Extracellular matrix hydrogel promotes tissue remodeling, arteriogenesis, and perfusion in a rat hindlimb ischemia model, JACC Basic Transl. Sci. 1 (2016) 32–44.
[64] Y. Fu, X. Fan, C. Tian, J. Luo, Y. Zhang, L. Deng, T. Qin, Q. Lv, Decellularization of porcine skeletal muscle extracellular matrix for the formulation of a matrix hydrogel: a preliminary study, J. Cell Mol. Med. 20 (2016) 740–749.
[65] H. Engel, S.W. Kao, J. Larson, S. Uriel, B. Jiang, E.M. Brey, M.H. Cheng, Investigation of Dermis-derived hydrogels for wound healing applications, Biomed. J. 38 (2015) 58–64.
[66] A. D'Amore, J.A. Stella, W.R. Wagner, M.S. Sacks, Characterization of the complete fiber network topology of planar fibrous tissues and scaffolds, Biomaterials 31 (2010) 5345–5354.
[67] D.A. Young, D.O. Ibrahim, D. Hu, K.L. Christman, Injectable hydrogel scaffold from decellularized human lipoaspirate, Acta Biomater. 7 (2011) 1040–1049.
[68] A. Engler, H. Sweeney, D. Discher, Matrix elasticity directs stem cell lineage specification, Cell 126 (2006) 677–689.
[69] M. Ahearne, A.P. Lynch, Early observation of extracellular matrix-derived hydrogels for corneal stroma regeneration, Tissue Eng. Part C Methods 21 (2015) 1059–1069.
[70] J. Wu, Q. Ding, A. Dutta, Y. Wang, Y.H. Huang, H. Weng, L. Tang, Y. Hong, An injectable extracellular matrix derived hydrogel for meniscus repair and regeneration, Acta Biomater. 16 (2015) 49–59.
[71] T.J. Keane, J. Dziki, A. Castelton, D.M. Faulk, V. Messerschmidt, R. Londono, J.E. Reing, S.S. Velankar, S.F. Badylak, Preparation and characterization of a biologic scaffold and hydrogel derived from colonic mucosa, J. Biomed. Mater. Res. B Appl. Biomater. (2015).
[72] M.J. Sawkins, W. Bowen, P. Dhadda, H. Markides, L.E. Sidney, A.J. Taylor, F.R. Rose, S.F. Badylak, K.M. Shakesheff, L.J. White, Hydrogels derived from demineralized and decellularized bone extracellular matrix, Acta Biomater. 9 (2013) 7865–7873.
[73] F. Pati, J. Jang, D.H. Ha, S. Won Kim, J.W. Rhie, J.H. Shim, D.H. Kim, D.W. Cho, Printing three-dimensional tissue analogues with decellularized extracellular matrix bioink, Nat. Commun. 5 (2014) 3935.
[74] J.M. Singelyn, K.L. Christman, Modulation of material properties of a decellularized myocardial matrix scaffold, Macromol. Biosci. 11 (2011) 731–738.
[75] J.M. Singelyn, J.A. DeQuach, S.B. Seif-Naraghi, R.B. Littlefield, P.J. Schup-Magoffin, K.L. Christman, Naturally derived myocardial matrix as an injectable scaffold for cardiac tissue engineering, Biomaterials 30 (2009) 5409–5416.
[76] S.B. Seif-Naraghi, D. Horn, P.A. Schup-Magoffin, M.M. Madani, K.L. Christman, Patient-to-patient variability in autologous pericardial matrix scaffolds for cardiac repair, J. Cardiovasc. Transl. Res. 4 (2011) 545–556.
[77] S.B. Seif-Naraghi, J.M. Singelyn, M.A. Salvatore, K.G. Osborn, J.J. Wang, U. Sampat, O.L. Kwan, G.M. Strachan, J. Wong, P.J. Schup-Magoffin, R.L. Braden, K. Bartels, J.A. DeQuach, M. Preul, A.M. Kinsey, A.N. DeMaria, N. Dib, K.L. Christman, Safety and efficacy of an injectable extracellular matrix hydrogel for treating myocardial infarction, Sci. Transl. Med. 5 (2013) 173ra25.
[78] S.B. Seif-Naraghi, D. Horn, P.J. Schup-Magoffin, K.L. Christman, Injectable extracellular matrix derived hydrogel provides a platform for enhanced retention and delivery of a heparin-binding growth factor, Acta Biomater. 8 (2012) 3695–3703.
[79] J.M. Singelyn, P. Sundaramurthy, T.D. Johnson, P.J. Schup-Magoffin, D.P. Hu, D. M. Faulk, J. Wang, K.M. Mayle, K. Bartels, M. Salvatore, A.M. Kinsey, A.N. Demaria, N. Dib, K.L. Christman, Catheter-deliverable hydrogel derived from decellularized ventricular extracellular matrix increases endogenous cardiomyocytes and preserves cardiac function post-myocardial infarction, J. Am. Coll. Cardiol. 59 (2012) 751–763.
[80] J.W. Wassenaar, R.L. Braden, K.G. Osborn, K.L. Christman, Modulating in vivo degradation rate of injectable extracellular matrix hydrogels, J. Mater. Chem. B 4 (2016) 2794–2802.
[81] J.W. Wassenaar, R. Gaetani, J.J. Garcia, R.L. Braden, C.G. Luo, D. Huang, A.N. DeMaria, J.H. Omens, K.L. Christman, Evidence for mechanisms underlying the functional benefits of a myocardial matrix hydrogel for post-MI treatment, J. Am. Coll. Cardiol. 67 (2016) 1074–1086.
[82] D. Tukmachev, S. Forostyak, Z. Koci, K. Zaviskova, I. Vackova, K. Vyborny, I. Sandvig, A. Sandvig, C.J. Medberry, S.F. Badylak, E. Sykova, S. Kubinova, Injectable extracellular matrix hydrogels as scaffolds for spinal cord injury repair, Tissue Eng. Part A 22 (2016) 306–317.
[83] J. Dequach, J. Lin, C. Cam, D. Hu, M. Salvatore, F. Sheikh, K. Christman, Injectable skeletal muscle matrix hydrogel promotes neovascularization and muscle cell infiltration in a hindlimb ischemia model, Eur. Cell Mater. 23 (2013) 400–412.
[84] M.Y. Kim, S. Farnebo, C.Y. Woon, T. Schmitt, H. Pham, J. Chang, Augmentation of tendon healing with an injectable tendon hydrogel in a rat Achilles tendon model, Plast. Reconstr. Surg. 133 (2014) 645e–653e.
[85] S. Ravi, J.M. Caves, A.W. Martinez, J. Xiao, J. Wen, C.A. Haller, M.E. Davis, E.L. Chaikof, Effect of bone marrow-derived extracellular matrix on cardiac function after ischemic injury, Biomaterials 33 (2012) 7736–7745.
[86] F. Paduano, M. Marrelli, L.J. White, K.M. Shakesheff, M. Tatullo, Odontogenic differentiation of human dental pulp stem cells on hydrogel scaffolds derived from decellularized bone extracellular matrix and collagen type I, PLoS ONE 11 (2016) e0148225.
[87] T.L. Sellaro, A.K. Ravindra, D.B. Stolz, S.F. Badylak, Maintenance of hepatic sinusoidal endothelial cell phenotype in vitro using organ-specific extracellular matrix scaffolds, Tissue Eng. 13 (2007) 2301–2310.
[88] T.L. Sellaro, A. Ranade, D.M. Faulk, G.P. McCabe, K. Dorko, S.F. Badylak, S.C. Strom, Maintenance of human hepatocyte function in vitro by liver-derived extracellular matrix gels, Tissue Eng. Part A 16 (2010) 1075–1082.
[89] S.F. Badylak, T.W. Gilbert, Immune response to biologic scaffold materials, Semin. Immunol. 20 (2008) 109–116.
[90] B.M. Sicari, J.L. Dziki, B.F. Siu, C.J. Medberry, C.L. Dearth, S.F. Badylak, The promotion of a constructive macrophage phenotype by solubilized extracellular matrix, Biomaterials 35 (2014) 8605–8612.

[91] F.W. Meng, P.F. Slivka, C.L. Dearth, S.F. Badylak, Solubilized extracellular matrix from brain and urinary bladder elicits distinct functional and phenotypic responses in macrophages, Biomaterials 46 (2015) 131–140.
[92] I. Ventrix, A Study of VentriGel in Early and Late Post-myocardial Infarction Patients, ClinicalTrials.gov [Internet], Bethseda, MD.
[93] R.M. Wang, K.L. Christman, Decellularized myocardial matrix hydrogels: in basic research and preclinical studies, Adv. Drug Deliv. Rev. 96 (2016) 77–82.
[94] S.B. Sonnenberg, A.A. Rane, C.J. Liu, N. Rao, G. Agmon, S. Suarez, R. Wang, A. Munoz, V. Bajaj, S. Zhang, R. Braden, P.J. Schup-Magoffin, O.L. Kwan, A.N. DeMaria, J.R. Cochran, K.L. Christman, Delivery of an engineered HGF fragment in an extracellular matrix-derived hydrogel prevents negative LV remodeling post-myocardial infarction, Biomaterials 45 (2015) 56–63.
[95] E.L. Smith, J.M. Kanczler, D. Gothard, C.A. Roberts, J.A. Wells, L.J. White, O. Qutachi, M.J. Sawkins, H. Peto, H. Rashidi, L. Rojo, M.M. Stevens, A.J. El Haj, F.R. Rose, K.M. Shakesheff, R.O. Oreffo, Evaluation of skeletal tissue repair, part 2: enhancement of skeletal tissue repair through dual-growth-factor-releasing hydrogels within an ex vivo chick femur defect model, Acta Biomater. 10 (2014) 4197–4205.
[96] A. Viswanath, J. Vanacker, L. Germain, J.G. Leprince, A. Diogenes, K. Shakesheff, L.J. White, A. Des Rieux, Extracellular matrix-derived hydrogels for dental stem cell delivery, J. Biomed. Mater. Res. A (2016).
[97] C.Y. Lin, T.Y. Liu, M.H. Chen, J.S. Sun, M.H. Chen, An injectable extracellular matrix for the reconstruction of epidural fat and the prevention of epidural fibrosis, Biomed. Mater. 11 (2016) 035010.
[98] D. Gothard, E.L. Smith, J.M. Kanczler, C.R. Black, J.A. Wells, C.A. Roberts, L.J. White, O. Qutachi, H. Peto, H. Rashidi, L. Rojo, M.M. Stevens, A.J. El Haj, F.R. Rose, K.M. Shakesheff, R.O. Oreffo, In vivo assessment of bone regeneration in alginate/bone ECM hydrogels with incorporated skeletal stem cells and single growth factors, PLoS ONE 10 (2015) e0145080.
[99] P.M. Crapo, S. Tottey, P.F. Slivka, S.F. Badylak, Effects of biologic scaffolds on human stem cells and implications for CNS tissue engineering, Tissue Eng. Part A 20 (2014) 313–323.
[100] D. Sood, K. Chwalek, E. Stuntz, D. Pouli, C. Du, M. Tang-Schomer, I. Georgakoudi, L.D. Black, D.L. Kaplan, Fetal brain extracellular matrix boosts neuronal network formation in 3D bioengineered model of cortical brain tissue, ACS Biomater. Sci. Eng. 2 (2016) 131–140.
[101] T.J. Keane, A. DeWard, R. Londono, L.T. Saldin, A.A. Castleton, L. Carey, A. Nieponice, E. Lagasse, S.F. Badylak, Tissue-specific effects of esophageal extracellular matrix, Tissue Eng. Part A 21 (2015) 2293–2300.
[102] W.L. Stoppel, D. Hu, I.J. Domian, D.L. Kaplan, L.D. Black 3rd., Anisotropic silk biomaterials containing cardiac extracellular matrix for cardiac tissue engineering, Biomed. Mater. 10 (2015) 034105.
[103] T.D. Johnson, R.L. Braden, K.L. Christman, Injectable ECM scaffolds for cardiac repair, Methods Mol. Biol. 1181 (2014) 109–120.
[104] J.L. Ungerleider, T.D. Johnson, N. Rao, K.L. Christman, Fabrication and characterization of injectable hydrogels derived from decellularized skeletal and cardiac muscle, Methods 84 (2015) 53–59.
[105] R. Gaetani, C. Yin, N. Srikumar, R. Braden, P.A. Doevendans, J.P. Sluijter, K.L. Christman, Cardiac derived extracellular matrix enhances cardiogenic properties of human cardiac progenitor cells, Cell Transplant. (2015).
[106] G.N. Grover, N. Rao, K.L. Christman, Myocardial matrix-polyethylene glycol hybrid hydrogels for tissue engineering, Nanotechnology 25 (2014) 014011.
[107] J. Jang, T.G. Kim, B.S. Kim, S.W. Kim, S.M. Kwon, D.W. Cho, Tailoring mechanical properties of decellularized extracellular matrix bioink by vitamin B2-induced photo-crosslinking, Acta Biomater. 33 (2016) 88–95.
[108] D.O. Freytes, J.D. O'Neill, Y. Duan-Arnold, E.A. Wrona, G. Vunjak-Novakovic, Natural cardiac extracellular matrix hydrogels for cultivation of human stem cell-derived cardiomyocytes, Methods Mol. Biol. 1181 (2014) 69–81.
[109] W.L. Stoppel, A.E. Gao, A.M. Greaney, B.P. Partlow, R.C. Bretherton, D.L. Kaplan, L.D. Black 3rd., Elastic, silk-cardiac extracellular matrix hydrogels exhibit time-dependent stiffening that modulates cardiac fibroblast response, J. Biomed. Mater. Res. A (2016).
[110] A. D'Amore, T. Yoshizumi, S.K. Luketich, M.T. Wolf, X. Gu, M. Cammarata, R. Hoff, S.F. Badylak, W.R. Wagner, Bi-layered polyurethane – extracellular matrix cardiac patch improves ischemic ventricular wall remodeling in a rat model, Biomaterials 107 (2016) 1–14.
[111] B. Kappler, P. Anic, M. Becker, A. Bader, K. Klose, O. Klein, B. Oberwallner, Y.H. Choi, V. Falk, C. Stamm, The cytoprotective capacity of processed human cardiac extracellular matrix, J. Mater. Sci. - Mater. Med. 27 (2016) 120.
[112] K. Fujita, Y. Tuchida, H. Seki, T. Kosawada, Z. Feng, D. Sat, T. Nakamura, Y. Shiraishi, M. Umezu, Characterizing and modulating the mechanical properties of hydrogels from ventricular extracellular matrix, IEEE (2015) 1–5.
[113] S. Seif-Naraghi, J. Singelyn, J. Dequach, P. Schup-Magoffin, K. Christman, Fabrication of biologically derived injectable materials for myocardial tissue engineering, J. Vis. Exp. (2010).
[114] D.M. Faulk, R. Londono, M.T. Wolf, C.A. Ranallo, C.A. Carruthers, J.D. Wildemann, C.L. Dearth, S.F. Badylak, ECM hydrogel coating mitigates the chronic inflammatory response to polypropylene mesh, Biomaterials 35 (2014) 8585–8595.
[115] M.T. Wolf, C.A. Carruthers, C.L. Dearth, P.M. Crapo, A. Huber, O.A. Burnsed, R. Londono, S.A. Johnson, K.A. Daly, E.C. Stahl, J.M. Freund, C.J. Medberry, L.E. Carey, A. Nieponice, N.J. Amoroso, S.F. Badylak, Polypropylene surgical mesh coated with extracellular matrix mitigates the host foreign body response, J. Biomed. Mater. Res. A 102 (2014) 234–246.
[116] M.T. Wolf, C.L. Dearth, C.A. Ranallo, S.T. LoPresti, L.E. Carey, K.A. Daly, B.N. Brown, S.F. Badylak, Macrophage polarization in response to ECM coated polypropylene mesh, Biomaterials 35 (2014) 6838–6849.